ISSN 1024-8560, Atmospheric and Oceanic Optics, 2021, Vol. 34, No. 2, pp. 128–133. © Pleiades Publishing, Ltd., 2021.
Russian Text © The Author(s), 2020, published in Optika Atmosfery i Okeana.

ATMOSPHERIC RADIATION, OPTICAL WEATHER, AND CLIMATE

The Relationship between the Ultraviolet Radiation and Meteorological Factors and Atmospheric Turbidity: Part II. Role of Surface Albedo

B. D. Belan[a], *, G. A. Ivlev[a], and T. K. Sklyadneva[a]

[a] *V.E. Zuev Institute of Atmospheric Optics, Siberian Branch, Russian Academy of Sciences, Tomsk, 634055 Russia*

**e-mail: bbd@iao.ru*

Received July 16, 2020; revised July 16, 2020; accepted October 26, 2020

Abstract—We analyze the interrelation between variations in the surface ultraviolet radiation in the wavelength range 280–320 nm and the state of the underlying surface. This is done using a homogeneous time series of measurements of UV–B radiation at the Tropospheric Ozone Research (TOR) station of the Institute of Atmospheric Optics, Siberian Branch, Russian Academy of Sciences, the atmospheric infrared sounder (AIRS) data on columnar ozone, ground-based aerosol optical depth (AOD) measurements from the AERONET network, and data on cloud cover available from the Institute of Monitoring of Climatic and Ecological Systems, Siberian Branch, Russian Academy of Sciences (IMCES SB RAS) meteorological site for 2004–2016.

Keywords: atmosphere, ultraviolet radiation, total ozone content, clouds, variations, albedo of the underlying surface

DOI: 10.1134/S1024856021020020

INTRODUCTION

Solar radiation drives most processes on the Earth. Global warming, observed in recent decades, is a reason for careful attention to the trends in variations in the solar radiation. The available data do not provide unambiguous estimates [1–3]. In works [1, 2], the trend over the past decade is shown to be at a level of 0.5–0.6 W m^{-2}. Estimates in [3] for this same period had been 2.0 W m^{-2}. This ambiguity in the total solar radiative flux requires an analysis of the behavior of its components in separate spectral regions and, in particular, variations in ultraviolet part of the flux, which determines photochemical and biological processes.

In work [4], we considered how the total ozone content (TOC) and aerosol optical depth (AOD) influence the variations in daily surface ultraviolet radiation in the wavelength range 280–320 nm (henceforth UV–B radiation) in Tomsk; it was found that a 1% TOC increase leads, on average, to a 1.45% decrease in the UV–B radiation under clear sky and high atmospheric transparency (total cloud amount (N_{total}) ≤ 2, $\text{AOD}_{500} \le 0.15$). It was noted that, depending on the cloud amount, the average contribution of AOD to variations in daily UV–B radiation is from 4.3 to 10.9%; the increment of UV–B radiation can, on average, decrease by 0.7–28.7%, if we consider that the average daily UV–B radiation under the clear-sky conditions is 31.2% larger than the total average values.

The authors of work [4] disregarded the effect of the albedo of the underlying surface, which can also make a substantial contribution to variations of the dependence of UV–B radiation on TOC. The variability range of the albedo of the underlying surface is quite wide and depends on the surface type. The albedo is 52–99% for snow cover, 12–28% for grass cover, 5–15% for dark soil, and 5–20% for forest [5–7]. It is noteworthy that the albedo of moist snow is 2–8% lower than the albedo of dry snow; the albedo of wet grass is 2–3% lower than the albedo of dry grass; and the albedo of moist soil is 3–8% lower than the albedo of dry soil. Therefore, the contribution of surface albedo to variations in UV–B radiation depends on the season and geographic position of the measurement site. Data in work [8] indicate that the snow cover increases the monthly doses of erythemal radiation by more than 20% in spring at high latitudes, where the Earth's surface is covered by snow for most of the year. The authors of work [9] analyzed the variations in UV–B radiation at λ = 305 nm over 1994–2006 at Sonnblick observatory (47.03° N, 12.57° E, 3106 m above sea level). It was shown that the maximal variations, caused by the albedo effect, reach 32% in April (6%, on average) and 12–15% in summer (3%, on average). Authors of work [10] estimated shortwave radiative forcing under clear-sky conditions. It was shown that this forcing is 120 W m^{-2} for an albedo in the range from 0.1 to 0.2, and it is 41 W m^{-2} for an albedo in

the range from 0.5 to 0.6. Based on data in [11], the ratio of scattered to total UV radiation varies from 78–80% in summer months to 96–99% in winter months, when snow cover is present.

In this paper, we analyze how the variations in surface ultraviolet radiation in the wavelength range 280–320 nm depend on the state of the underlying surface in the region of measurements. A long-term time series of hourly measurements of UV–B radiation for 2004–2016, obtained at the Tropospheric Ozone Research (TOR) station of the Institute of Atmospheric Optics, Siberian Branch, Russian Academy of Sciences (IAO SB RAS) [12], was taken as initial data. As in [4], the variability factors of UV–B radiation were analyzed using AOD_{500} data, obtained from ground-based measurements of direct radiation by a CE-318 photometer within the AERONET network in Tomsk (https://aeronet.gsfc.nasa.gov; 2.0 processing level data). The results from Atmospheric Infrared Sounder (AIRS) monitoring of columnar aerosol content were taken from http://giovanni.gsfc.nasa.gov. Additionally, we employed information on the amount of snow cover in the region of measurements provided by personnel of meteorological station in the Institute of Monitoring of Climatic and Ecological Systems, Siberian Branch, Russian Academy of Sciences (IMCES SB RAS).

PREPARATION OF INITIAL DATA FOR CALCULATIONS

Over the period under study (2004–2016), Tomsk was repeatedly covered by smokes from forest fires on the territories of Tomsk and nearby regions. The smoke pollution was the strongest during summers 2012 and 2016, which influenced the AOD and the magnitude of the surface UV–B radiation. Therefore, we excluded the smoke situations (according to the $AOD_{500} > 0.3$ criterion) from the total dataset. The threshold value was chosen taking into account the annual behavior of AOD_{500} in 1995–2018 in Tomsk without smokes [13]. In all, 195 cases of measurements of surface UV–B radiation were sorted out. A "measurement case" is taken to mean hourly arithmetically average flux of UV–B radiation, obtained after averaging 600 measurements taken every second at the beginning of every hour 24 times a day.

The measurements thus selected were then categorized into two groups: "snow-covered" (in the presence of snow cover) and "snow-free" (in the absence of snow) measurements.

The analysis of data on the state of snow cover over the years of measurements of UV–B radiation at the TOR station, IAO SB RAS, showed that snow cover in Tomsk becomes stable on November 15, on the average, and remains so until April 15. The periods from October 1 to November 15, and from April 15 to May 1 can be considered as transitional, when snow cover amount is less than 10 points and surface albedo varies as a function of the degree of snow coverage of soil and the degree of variability of forest in the region of the TOR station. The dynamics of the snow cover depth is characterized by sharp jump-like variations during a transitional period. Strong thaws favor the formation of thawed patches and decreases in snow depth; while passing cyclones and associated snowfalls are responsible for a sharp increase in the snow cover depth and albedo [14]. In this period, the albedo difference between neighboring days may reach 20–30%. The underlying surface is more homogeneous in winter and summer. This difference does not exceed 3% in summer; and it is <7% in winter at midlatitudes with a continental climate [15]. Therefore, we considered situations with stable (snow-covered and snow-free) states of the underlying surface. The snow-covered sample was compiled to include November, February, March, and April (until April 15). December and January were out of the sampling period because, in view of the constraint on the solar zenith angle (SZA) ($50° \le Z < 74°$). The SZA does not reach values from the above range in these months.

Then, the values selected were divided into subsets according to SZA ($M \le Z \ll (M + 2°)$) at time of radiation measurement within the observed range $50° \le Z < 74°$. The boundaries of the total SZA range were determined taking into account the fact that angles, close to 50° are limiting for the cases of UV–B radiation measurements in the presence of snow cover. For smaller SZA, the number of cases becomes statistically negligible. In the analysis below, the results obtained in this work and in [4] are to be used to analyze the behavior of separate spectral regions of shortwave radiation; therefore, we chose the upper boundary of 74° taking into account the fact that the Brewer spectrophotometer, available to us (which can be used for TOC and UV–B radiation measurements), cannot determine the TOC for $Z > 75°$. In both groups, we identified subsets with different TOC (200–300, 300–400, and 400–500 DU) values. Only eight cases with snow and no snow-free cases fell within the range 500–600 DU. Therefore, this TOC variability range is not considered here.

To eliminate the cloud effect, the total dataset was processed to extract a subset of data under clear-sky conditions ($N_{total} = 0$) taking into account the above constraints. This subset comprised 1717 measurement cases over the entire period of measurements. We have also analyzed how the situation changes if cases with the cloud amount equal to 1–2 are added to the available clear-sky cases. A comparison of the average values of UV–B radiation for $N_{total} = 0$ (N_0) and $N_{total} = 0–2$ ($N_{0–2}$) and for different TOC values showed that variations in UV–B radiation throughout SZA range did not exceed 6% when we considered not only the clear-sky cases, but also cases with the cloud amount up to 2. Thus, the number of cases in the data subset,

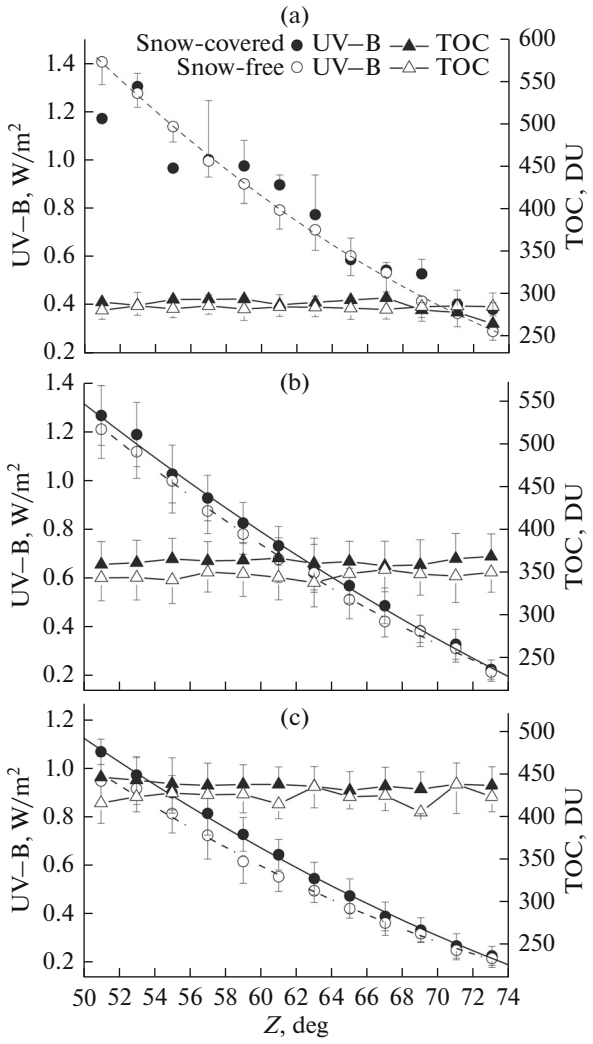

Fig. 1. Dependence of UV–B radiation on solar zenith angle for (a) TOC = 200–300, (b) 300–400, and (c) 400–500 DU. Second-order polynomial fits are presented for UV–B radiation. Circles and triangles indicate the averages of measurements; error bars show standard deviations; N_{total} = 0–2 cloud amount, AOD < 0.3.

selected for the analysis, increased to 2505 (1011 snow-covered cases and 1494 snow-free cases). As can be seen from Table 1, the differences are maximal for the range TOC = 200–300 DU, in which either no suitable observation cases were available, or separate cases were noted, for the series of two-degree SZA ranges. For the other TOC ranges, the deviations of values are within the errors of the measuring instruments. Therefore, the dataset obtained for N_{total} = 0–2 is used below.

RESULTS AND ANALYSIS

The dataset thus compiled was used to calculate the average values of UV–B radiation in the presence and absence of snow cover for different TOC and SZA variability ranges (Table 2).

Figure 1 shows how values of UV–B radiation vary versus SZA in different TOC and surface albedo ranges (in the presence and absence of snow cover). Figures 1b and 1c indicate that variations in UV–B radiation are well fitted by a second-order polynomial (determination coefficient R^2 = 0.99) in the ranges TOC = 300–400 and 400–500 DU. The pattern is different for TOC = 200–300 DU (Fig. 1a): the variations in UV–B radiation are also well fitted by a second-order polynomial in the absence of snow cover, and not so in the presence of snow cover (because of poor statistical representativeness); therefore, it seems no regularities can be identified on the basis of data from field measurements for this TOC range.

Thus, for the data of field measurements used here we derived a nonlinear relationship UV–B = $a_1Z^2 + a_2Z + b$ (Table 3) between the radiation intensity and SZA for different ranges of TOC and state of the underlying surface.

We estimated the increment of UV–B radiation in the presence of snow (Fig. 2) by the formula

$$\Delta = (\mathrm{UV\text{–}B_1} - \mathrm{UV\text{–}B_2})/\mathrm{UV\text{–}B_2} \times 100\%,$$

Table 1. Variations in UV–B radiation as the cloud amount increases to 2, $\Delta = (N_{0-2} - N_0)/N_0 \times 100\%$

Z, deg	TOC, DU					
	200–300		300–400		400–500	
	snow-covered	snow-free	snow-covered	snow-free	snow-covered	snow-free
50–52	–	−0.4	0.9	0	0.8	0
52–54	3.8	−1.2	0.8	0	2.5	−7.1
54–56	–	0.6	1.1	0	3.7	5.6
56–58	20.9	0.4	0.3	2.4	6.3	−9.8
58–60	4.1	0.0	0	1.8	2.1	1.8
60–62	1.2	1.4	0.4	2.0	−4.7	0.5
62–64	8.7	1.3	0.8	3.0	1.3	4.7
64–66	9.3	−1.8	−0.7	2.7	−1.1	−4.9
66–68	7.3	3.2	4.9	1.7	3.4	1.8
68–70	5.8	2.8	1.3	2.6	1.8	0
70–72	0.7	−0.8	4.8	5.2	2.3	0
72–74	0.5	0.7	0.8	1.2	0.4	4.3

Table 2. Averages and standard deviations (σ) of UV–B radiation and TOC under snow-covered and snow-free conditions for different zenith angles at $N_{total} = 0–2$, $AOD_{500} < 0.3$

Z, deg	Snow-covered				Snow-free		
	TOC, DU	number of cases	UV–B ± σ, W/m^2	TOC ± σ, DU	number of cases	UV–B ± σ, W/m^2	TOC ± σ, DU
50–52	200–300	–	–	–	19	1.406 ± 0.094	279.76 ± 10.70
	300–400	20	1.265 ± 0.122	359.08 ± 26.78	111	1.209 ± 0.119	343.40 ± 26.71
	400–500	25	1.064 ± 0.052	445.57 ± 24.10	3	0.944 ± 0.091	415.27 ± 23.81
52–54	200–300	3	1.304 ± 0.054	285.79 ± 5.26	18	1.276 ± 0.058	285.00 ± 11.11
	300–400	34	1.187 ± 0.131	361.09 ± 26.20	81	1.117 ± 0.108	343.78 ± 26.11
	400–500	29	0.968 ± 0.076	442.12 ± 26.51	3	0.913 ± 0.065	422.63 ± 17.63
54–56	200–300	1	0.966	292.57	25	1.138 ± 0.064	281.49 ± 10.53
	300–400	34	1.026 ± 0.118	365.56 ± 23.83	52	0.998 ± 0.131	341.01 ± 27.45
	400–500	20	0.896 ± 0.071	437.72 ± 30.60	5	0.810 ± 0.079	426.99 ± 23.43
56–58	200–300	2	1.001 ± 0.245	292.94 ± 5.03	26	0.996 ± 0.067	285.08 ± 10.01
	300–400	24	0.928 ± 0.093	363.23 ± 22.68	116	0.875 ± 0.092	349.94 ± 22.99
	400–500	33	0.811 ± 0.089	435.82 ± 26.20	10	0.721 ± 0.096	424.99 ± 18.84
58–60	200–300	3	0.975 ± 0.106	293.01 ± 0.38	30	0.900 ± 0.080	281.16 ± 13.34
	300–400	37	0.826 ± 0.084	364.08 ± 20.67	108	0.781 ± 0.083	348.28 ± 26.38
	400–500	36	0.725 ± 0.069	437.17 ± 23.07	6	0.615 ± 0.089	425.58 ± 21.72
60–62	200–300	5	0.897 ± 0.042	286.34 ± 11.81	27	0.787 ± 0.086	283.72 ± 10.85
	300–400	36	0.733 ± 0.079	366.51 ± 23.86	80	0.678 ± 0.095	343.98 ± 26.21
	400–500	36	0.642 ± 0.062	437.20 ± 20.46	5	0.553 ± 0.061	414.12 ± 17.09
62–64	200–300	2	0.867 ± 0.06	287.28 ± 9.71	36	0.726 ± 0.067	283.48 ± 11.70
	300–400	30	0.646 ± 0.093	360.25 ± 29.46	43	0.622 ± 0.079	337.86 ± 28.29
	400–500	54	0.545 ± 0.067	434.77 ± 23.36	4	0.495 ± 0.048	434.32 ± 24.57
64–66	200–300	3	0.589 ± 0.089	291.95 ± 2.22	31	0.604 ± 0.081	282.30 ± 13.43
	300–400	43	0.570 ± 0.071	362.46 ± 23.74	109	0.513 ± 0.078	348.20 ± 24.88
	400–500	48	0.474 ± 0.070	430.05 ± 22.14	12	0.422 ± 0.039	422.63 ± 14.30
66–68	200–300	3	0.545 ± 0.032	294.40 ± 1.98	36	0.535 ± 0.080	280.69 ± 11.37
	300–400	39	0.488 ± 0.073	357.52 ± 28.89	99	0.424 ± 0.063	353.16 ± 25.88
	400–500	39	0.390 ± 0.059	434.89 ± 22.21	4	0.363 ± 0.051	423.94 ± 17.72
68–70	200–300	9	0.530 ± 0.060	280.05 ± 8.84	31	0.433 ± 0.055	283.97 ± 13.35
	300–400	41	0.386 ± 0.064	358.48 ± 29.43	100	0.384 ± 0.046	347.84 ± 24.58
	400–500	66	0.334 ± 0.051	431.70 ± 20.23	3	0.319 ± 0.033	404.45 ± 1.57
70–72	200–300	9	0.404 ± 0.059	277.31 ± 15.95	30	0.368 ± 0.056	284.72 ± 10.77
	300–400	44	0.331 ± 0.061	365.73 ± 29.51	54	0.314 ± 0.056	345.50 ± 30.79
	400–500	55	0.269 ± 0.050	437.33 ± 24.94	8	0.251 ± 0.039	437.25 ± 34.15
72–74	200–300	21	0.383 ± 0.068	263.91 ± 24.86	29	0.292 ± 0.037	284.11 ± 10.90
	300–400	57	0.266 ± 0.053	368.43 ± 26.31	127	0.259 ± 0.049	350.04 ± 23.30
	400–500	70	0.228 ± 0.039	435.81 ± 21.89	13	0.218 ± 0.038	422.68 ± 17.65

Table 3. Coefficients a and b in the regression equation UV–B = $a_1Z^2 + a_2Z + b$

Coefficient	TOC, DU			
	300–400		400–500	
	snow-covered	snow-free	snow-covered	snow-free
a_1	4.16×10^{-4}	6.58×10^{-4}	4.54×10^{-4}	5.59×10^{-4}
a_2	-981.10×10^{-4}	-1262.00×10^{-4}	-951.50×10^{-4}	-1039.80×10^{-4}
b	5.18	5.94	4.74	4.82
R^2	0.998	0.998	0.999	0.996

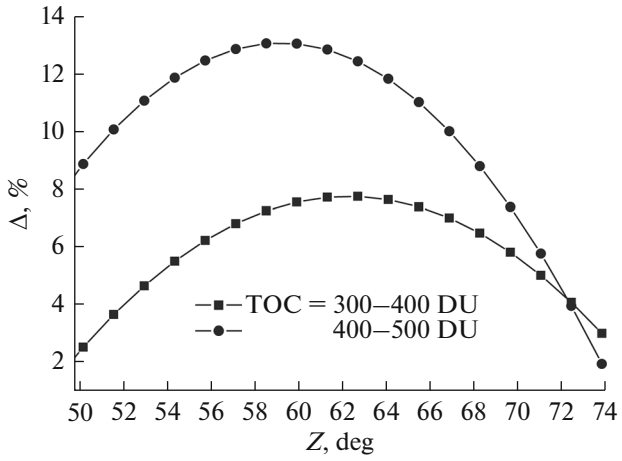

Fig. 2. Increment of UV–B radiation for a stable snow cover relative to the level of UV–B radiation for the snow-free underlying surface.

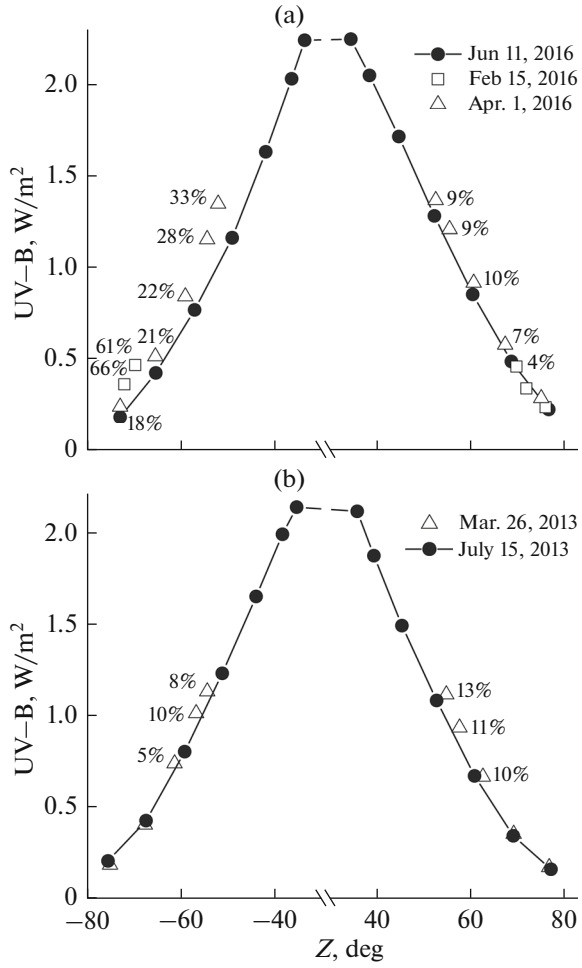

Fig. 3. Values of surface UV–B radiation. Numbers indicate percentage intensity increments for days with (a) fresh and (b) aged snow.

where $UV–B_1$ is the radiation for a stable snow cover; and $UV–B_2$ is UV–B radiation in the absence of snow cover.

Figure 2 indicates that the level of UV–B radiation for a stable snow cover on the underlying surface for SZA $52 < Z < 68°$ increases by 4–8% relative to the level of UV–B radiation in the absence of snow for TOC = 300–400 DU, and by 9–13%, for TOC = 400–500 DU. We also note that the average TOC values are higher for a stable snow cover than in the absence of snow (Fig. 1).

As is already indicated above, the albedo of snow cover varies from 52 to 99% and depends on the state of snow: the albedo of fresh dry snow is 85–95%; while albedos of polluted and dirty snow are 40–50% and 20–30%, respectively.

Figure 3a shows the variations in UV–B radiation on February 15 and April 1, 2016, as compared to those on June 11; and Fig. 3b shows these variations on March 26 as compared to those on July 15, 2013. On those days, TOC = 391 (February 15, 2016), 371 (April 1, 2016), 335 (June 11, 2016), 371 (March 26, 2013), and 348 DU (July 15, 2013).

In work [4], we have found that, when $N_{total} \le 2$ and $AOD_{500} \le 0.15$, an increase in TOC by 1% causes UV–B radiation to decrease by 1.45%. Therefore, the values of UV–B radiation were corrected relative to TOC = 335 DU (June 11, 2016) on February 15 and April 1, 2016, and relative to TOC = 348 DU (July 15, 2013) on March 26, 2013.

On February 15, 2016, the increase in UV–B radiation until noon due to the difference in surface albedo had been 61–66% (Fig. 3a). We note that there was a snowfall from February 5 to 12, 2016; therefore, the albedo on February 15 was close to values maximally possible for snow cover.

On April 1, 2016, the incoming UV–B radiation at the surface level increased due to surface albedo by 21–33% before noon, and by 10%, after noon because snow was dirty and compacted (there was rain on March 29, 2016, from 09:00 to 11:00 LT; and drizzle was observed toward evening). This case demonstrates how can moistening of snow cover and decrease in its albedo during daylight hours of a single day strongly affect the intensity of UV–B radiation.

On March 26, 2013, the contribution of surface albedo to an increase in UV–B radiation did not exceed 13% (Fig. 3b).

CONCLUSIONS

In the solar zenith angle range from 52° to 68°, the contribution of the increment of surface albedo to increased level of UV–B radiation is, on average, 4–8% for TOC = 300–400 DU and 9–13% for TOC = 400–500 DU provided that the snow cover is stable. For days with fresh snow, the increase in UV–B radiation may reach 66% for TOC = 300–400 DU.

FUNDING

This work was supported by the Russian Foundation for Basic Research (grant no. 19-05-50024). The grant works were implemented using the infrastructure of the Institute of Atmospheric Optics, Siberian Branch, Russian Academy of Sciences, created and operated within State Assignment no. AAAA-A17-117021310142-5, including the "Atmosphere" Common Use Center.

CONFLICT OF INTEREST

The authors declare that they have no conflicts of interest.

REFERENCES

1. K. E. Trenberth, J. Fasullo, and M. A. Balmaseda, "Earth's energy imbalance," J. Clim. **27** (9), 3129–3144 (2014).
2. G. L. Stephens and T. l'Ecuyer, "The Earth's energy balance," Atmos. Res. **166**, 195–203 (2015).
3. A. Sanchez-Lorenzo, A. Enriquez-Alonso, M. Wild, J. Trentmann, S. M. Vicente-Serrano, A. Sanchez-Romero, R. Posselt, and M. Z. Hakuba, "Trends in downward surface solar radiation from satellites and ground observations over Europe during 1983–2010," Remote Sens. Environ. **189**, 108–117 (2017).
4. B. D. Belan, G. A. Ivlev, and T. K. Sklyadneva, "The relationship between ultraviolet radiation and meteorological factors and atmospheric turbidity: Part I. Role of total ozone content, clouds, and aerosol optical depth," Atmos. Ocean. Opt. **33** (6), 638–644 (2020).
5. S. P. Khromov and L. I. Mamontova, *Meteorological Dictionary* (Gidrometeoizdat, Leningrad, 1974) [in Russian].
6. K. Ya. Kondratyev, *Radiation in the Atmosphere* (Academic Press, New York, London, 1969).
7. B. D. Belan and T. K. Sklyadneva, "Albedo of some types of the underlying surface in Western Siberia," Optika Atmos. Okeana **18** (8), 727–730 (2005).
8. A. Kylling, A. Dahlback, and B. Mayer, "The effect of clouds and surface albedo on UV irradiances at a high latitude site," Geophys. Rev. Lett. **27** (9), 1411–1414 (2000).
9. S. Simic, P. Weihs, A. Vacek, H. Kromp-Kolb, and M. Fitzka, "Spectral UV measurements in Austria from 1994 to 2006: Investigations of short- and long-term changes," Atmos. Chem. Phys., No. 8, 7033–7043 (2008).
10. C. Di Biagio, A. di Sarra, P. Eriksen, S. E. Ascanius, G. Muscari, and B. Holben, "Effect of surface albedo, water vapour, and atmospheric aerosols on the cloud-free shortwave radiative budget in the Arctic," Clim. Dyn. **39** (3-4), 953–969 (2012).
11. E. I. Nezval' and N. E. Chubarova, "Long-term variability of UV radiation in the spectral range of 300–380 nm in Moscow," Rus. Meteorol. Hydrol. **42** (11), 693–699 (2017).
12. D. K. Davydov, B. D. Belan, P. N. Antokhin, O. Yu. Antokhina, V. V. Antonovich, V. G. Arshinova, M. Yu. Arshinov, A. Yu. Akhlestin, S. B. Belan, N. V. Dudorova, G. A. Ivlev, A. V. Kozlov, D. A. Pestunov, T. M. Rasskazchikova, D. E. Savkin, D. V. Simonenkov, T. K. Sklyadneva, G. N. Tolmachev, A. Z. Fazliev, and A. V. Fofonov, "Monitoring of atmospheric parameters: 25 years of the tropospheric ozone research station of the Institute of Atmospheric Optics, Siberian Branch, Russian Academy of Sciences," Atmos. Ocean. Opt. **32** (2), 180–192 (2019).
13. D. M. Kabanov, S. M. Sakerin, and Yu. S. Turchinovich, "Interannual and seasonal variations in the atmospheric aerosol optical depth in the region of Tomsk (1995–2018)," Atmos. Ocean. Opt. **32** (6), 663–670 (2019).
14. *Ecological and Climatic Characterization of the Atmosphere in 2012 from MSU Observatory Data* (MAKS Press, Moscow, 2013) [in Russian].
15. B. P. Alisov and B. V. Poltaraus, *Climatology* (Moscow State University, Moscow, 1974) [in Russian].

Translated by O. Bazhenov